Effects of postural change from supine to head-up tilt on skin sympathetic nerve activity component synchronised with cardiac cycle in warmed men

Yu Ogawa*, Yoshi-ichiro Kamijo*,**, Shigeki Ikegawa, Shizue Masuki, and Hiroshi Nose

Department of Sports Medical Sciences, Shinshu University Graduate School of Medicine and Institute for Biomedical Sciences, Matsumoto 390-8621, Japan

Running head: Baroreflex control of SSNA

Field: Integrative Physiology

Word count: 6,414

Tables: 4

Figures: 7

This is an Accepted Article that has been peer-reviewed and approved for publication in the The Journal of Physiology, but has yet to undergo copy-editing and proof correction. Please cite this article as an 'Accepted Article'; doi: 10.1113/JP273281.

Address correspondence to:

Hiroshi Nose, M.D., Ph.D.

Department of Sports Medical Sciences,

Shinshu University Graduate School of Medicine and Institute for Biomedical Sciences.

Asahi 3-1-1, Matsumoto 390-8621, Japan

Phone: +81-263-37-2681; Fax: +81-263-34-6721

E-mail: nosehir@shinshu-u.ac.jp.

*Y. Ogawa and Y. Kamijo contributed equally to this work.

**The present address for Y. Kamijo is Department of Rehabilitation Medicine, Wakayama Medical University, 811-1 Kimiidera, Wakayama 641-8509, Japan.

Non-technical summary

- Humans are unique in controlling body temperature in a hot environment by a large amount of skin blood flow; however, the decrease in total peripheral resistance due to systemic cutaneous vasodilatation and the reduction of venous return to the heart due to blood pooling in the cutaneous vein threaten blood pressure maintenance in the upright position, and occasionally cause heat syncope.
- Against this condition, cutaneous vasodilatation is reportedly suppressed to maintain arterial pressure; however, the nerve activity responsible for these phenomena has not been identified.
- In the present study, we found that the skin sympathetic nerve activity component that was synchronised with the cardiac cycle increased in hyperthermia but the increase was suppressed when the posture was changed from supine to head-up tilt.
- The profile of the component agreed with that of cutaneous vasodilatation.
- Thus, the component might contribute to the prevention of heat syncope in humans.

ABSTRACT

In humans, the cutaneous vasodilatation response to hyperthermia has been suggested to be suppressed by baroreflexes to maintain arterial pressure when the posture was changed from supine to upright, and if the reflexes do not function sufficiently, it can cause heat

syncope. However, the efferent signals of the reflexes have not been identified. To identify the signals, we continuously measured skin sympathetic nerve activity (SSNA; microneurography), right atrial volume (RAV; echocardiography, the baroreceptors for the reflexes are reportedly located), cutaneous vascular conductance on the chest (CVC_{chest}; laser Doppler flowmetry), and oesophageal temperature (T_{oes}; thermocouple) in young men before and after passive warming with a perfusion suit, during which periods the posture was changed from supine to 30° head-up tilt positions. During these periods, we also simultaneously measured muscle sympathetic nerve activity (MSNA) to distinguish the SSNA from MSNA. We found that an increase in T_{oes} by ~0.7°C (P<0.0001) increased the total SSNA (P<0.005); however, the head-up tilt in hyperthermia did not change the total SSNA (P>0.26) although an increase in CVC_{chest} (P<0.019) was suppressed and RAV was reduced (P<0.008). In contrast, the SSNA component synchronised with the cardiac cycle increased in hyperthermia (P<0.015), but decreased with the postural change (P<0.017). The SSNA component during the postural change before and after warming was highly correlated with the CVC_{chest} (r=0.817, P<0.0001), but the MSNA component was not (r=0.359, P=0.085). Thus, the SSNA component synchronised with the cardiac cycle appeared to be involved in suppressing cutaneous vasodilatation during postural changes.

Key words: thermoregulation, skin blood flow, baroreflexes, head-up tilt

ABBREVIATIONS

CCAD, common carotid artery diameter;

CVC, cutaneous vascular conductance;

LA_{min}, the SSNA or MSNA spike component that is not synchronised with the cardiac cycle per minute;

MSNA, muscle sympathetic nerve activity;

RAV, right atrial volume;

SSNA, skin sympathetic nerve activity;

T_{CCAD}, the latency of the valley of the CCAD wave after an R-wave;

T_{oes}, oesophageal temperature;

T_R, a peak-to-peak interval for R-wave incidence histogram;

T_{RAV}, the latency of a peak RAV after an R-wave;

T_{RS}, the latency of a peak of SSNA or MSNA incidence curve after an R-wave;

T_S, the peak-to-peak interval time of SSNA- or MSNA- spike incidence histogram;

UA_{min}, the SSNA or MSNA spike component that is synchronised with the cardiac cycle per minute.

INTRODUCTION

In humans, skin blood flow increases with increases in body temperature during exposure to a hot environment; however, the total peripheral resistance decreases due to systemic cutaneous vasodilatation, and venous return to the heart also decreases due to blood pooling in the cutaneous vein, and if not compensated for, these responses threaten the maintenance of arterial blood pressure during postural changes from supine to upright positions (Lind *et al.* 1968), which can occasionally cause heat syncope (Crandall *et al.* 2010). Although one of the compensation mechanisms is the baroreflex-induced suppression of cutaneous vasodilatation, the associated efferent skin sympathetic nerve activity (SSNA) signals have not been identified (Cui *et al.* 2004).

Recently, Kamijo *et al*. (2011) reported in young men that the SSNA component that was synchronised with the cardiac cycle increased as the oesophageal temperature (T_{oes}) increased with cutaneous vasodilatation during passive warming; however, the increase in the component was suppressed with reduced cutaneous vasodilatation by hypovolaemia which was induced by the administration of a diuretic prior to the warming. These results suggest that the component is the active vasodilator system, which causes hyperthermia-induced cutaneous vasodilatation, but this system is suppressed by unloading of baroreceptors. However, the results were obtained during prolonged and steady hypovolaemia stimulation to the mechanoreceptors. Thus, it remains unknown whether these mechanisms function also in situations requiring more rapid suppression of cutaneous vasodilatation such as when the

posture is changed from supine to upright. The first aim of the present study was to address this issue.

The second aim of this study was to examine the idea that atrial rather than arterial distension triggers the burst of the SSNA component. It has been suggested that cutaneous vasodilatation is modulated by atrial rather than arterial baroreceptors in hyperthermic humans (Ahmad *et al.* 1977; Mack *et al.* 1988; Crandall *et al.* 1996; Nagashima *et al.* 1998). Additionally, we previously suggested that the peak spike incidence of the SSNA component agreed with the timing of atrial filling rather than carotid arterial wall distension based on estimations from ECG profiles (Kamijo *et al*. 2011). This notion contrasts with the case of the muscle sympathetic nerve activity (MSNA) component for which burst timing agrees with the timing of the deflation of the common carotid artery (Kienbaum *et al.* 2001). However, a more precise assessment of this issue required more direct measures of the latencies of the SSNA and MSNA components following changes in atrial volume or carotid arterial diameter during the cardiac cycle and comparison of these latencies with those that have previously been reported (Fagius & Wallin, 1980).

Based on this background, we examined the following hypotheses in the present study: 1) the SSNA component increases with increases in body temperature, but this increase is suppressed with postural changes from supine to head-up tilt positions; 2) the profile of cutaneous vascular conductance during the postural changes before and after warming agree with the changes in the SSNA component and not the MSNA component; and 3) the SSNA component is triggered by atrial rather than arterial distension during the cardiac cycle when considering the burst timing of the SSNA as previously reported (Fagius & Wallin, 1980).

Results supporting these hypotheses would suggest that the SSNA component synchronised with the cardiac cycle is the active vasodilator that controls skin blood flow during hyperthermia, and this activity is suppressed by the unloading of atrial baroreceptors when the posture is changed from a supine to a head-up tilt position possibly to prevent heat syncope.

METHODS

Subjects

The procedures in this study conformed to the guidelines of the Declaration of Helsinki and were approved by the Review Board on Human Experiments of Shinshu University School of Medicine. After the experimental protocol had been fully explained, twelve young male volunteers provided their written informed consent before participating in this study. The physical characteristics of the subjects were as follows: 25 ± 6 (means ± SD) years of age, 172 ± 5 cm in height, 66 ± 7 kg in body weight, and peak oxygen consumption rate of 48.8 ± 7.7 ml kg^{-1} min^{-1}. All subjects were nonsmokers with no histories of cardiovascular or pulmonary diseases. Female subjects were excluded from this study because thermoregulatory and cardiovascular responses to orthostatic and thermal stress are reportedly affected by the menstrual cycle (Minson *et al.* 2000; Tanaka *et al.* 2003).

Experimental protocol

We determined peak oxygen consumption rate for each subject using graded cycling exercise more than 3 days before the experiment. On the experimental day, the subjects were asked to refrain from consuming caffeine or alcohol and from performing high-intensity exercise for 24 hours before the experiment. The subjects reported to the laboratory at 0700 in a normally hydrated state after fasting for more than 10 hours before the experiment. After emptying their bladders, the subjects were weighed in the nude and wore short pants and a tube-lined perfusion suit that covered all of the skin except for the face, hands, and calf, from which the SSNA and MSNA were measured. The subjects then entered an artificial climate chamber that was adjusted to an atmospheric temperature of 28.4 [26.2 – 30.2] °C and a relative humidity of 26.0 [12.6 – 42.3] % (means [min. – max.]) and were in the left posterior oblique position during the application of the measurement devices.

During normothermia before the warming, 10-min baseline measurements of the SSNA, MSNA, mean skin temperature, T_{oes}, heart rate (HR), skin blood flow on the chest and the dorsal foot, sweat rate on the dorsal foot, and blood pressure were acquired with the subjects in the supine position while 34°C water was perfused through the suit. During the 10-min measurement period, we performed right atrial volume (RAV) and common carotid arterial diameter (CCAD) measurements over 5 heartbeats using an ultrasound system (Vivid 7, General Electric, Fairfield, CT, USA).

After the 10-min measurement period in the supine position, the tilt table was inclined to 30° at a speed of 0.5° s^{-1}. A saddle was used to maintain the hip position so that the body did not slide down and the legs were not weighted. Next, we performed the same measurements over 10 min in the head-up tilt position.

Thereafter, the subjects were returned to the supine position, and 47°C water was perfused through the suit to warm the body. We confirmed that the T_{oes} increased and reached a steady state after 45 – 73 min of perfusion, during which time the T_{oes} increased by less than 0.05°C in 5 min. Subsequently, the 10-min measurement periods were repeated in the supine and 30° head-up-tilt positions.

No subjects suffered from syncopal events during the procedure. After the measurements, we determined the maximal skin blood flow by heating a skin site to which a probe was attached to ~42°C for 30 min using incandescent lamps to normalise the inter-individual variation in the maximal skin blood flow.

Measurements

Microneurography:

A tungsten microelectrode with an impedance of 4 MΩ at 1k Hz, a 35-mm length, a < 5-μm tip, and a 200-μm shank diameter was inserted percutaneously into the cutaneous nerve fascicles in the superficial peroneal nerve at the posterior aspect of the head of the fibula to record multiple-unit postganglionic SSNAs. To set a reference, an Ag-AgCl electrode (Vitrode Bs; Nihon Kohden Corp., Tokyo, Japan) was attached on the surface of the skin ~5 cm from the recording electrode. The nerve signal was pre-amplified by 10000-fold (DAM80; WPI Inc., Sarasota, FL, USA), transferred to a digital tape recorder, and passed through a band-pass filter of 700 – 2000 Hz. Next, the signal was sent to a loud speaker and sent in parallel to a resistance-capacitance circuit to rectify and filter the signal with time

constant (τ) 0.1 s. Another microelectrode was inserted into the skin 2 – 3 cm proximal to the SSNA electrode to obtain the MSNA signal, which was transferred to the same recording system as the SSNA.

We confirmed that the signals met the following criteria for an SSNA: 1) the subjects felt paraesthesia in the dorsal foot without any numbness; 2) a sympathetic burst was evoked by a deep breath, sudden arousal or gentle touch within the innervated area; and 3) no sympathetic burst was evoked by Valsalva's manoeuvre (Delius *et al.* 1972c). In contrast, the criteria for identifying an MSNA burst were spontaneous discharges that were 1) synchronised with the heartbeat; 2) enhanced by the Valsalva's manoeuvre; and 3) unchanged in response to cutaneous touch or arousal stimuli (Delius *et al.* 1972a, b; Vallbo *et al.* 1979). We failed to record either SSNA or MSNA in 6 of the 12 subjects because an electrode tip fell out of the fascicles of the nerves during the measurements. Thus, we analysed the SSNAs and MSNAs from the 6 subjects from whom we successfully recorded both signals.

T_{oes}, skin temperature, skin blood flow, and sweat rate:

T_{oes} was monitored using a thermocouple as described in our previous study (Kamijo *et al*. 2011). The skin temperatures were also measured with thermocouples at seven sites, and mean skin temperature was calculated as reported (Crawshaw *et al.* 1975).

Skin blood flow was measured by laser Doppler velocimetry (τ = 0.1 s; moorVMS-LDF2; Moor instruments, Devon, UK) on the chest and on the dorsal foot. The reason for the measurement of skin blood flow at the two sites is that the cutaneous vasodilatation on the

dorsal foot would be reportedly reduced during head-up tilt not only by the baroreflex control of the SSNA but also by the venoarteriolar reflex, which is a local axon-reflex. The latter reflex is stimulated by the venous wall stretching that occurs as the hydrostatic pressure increases due to venous blood stasis in the head-up tilt position (Rowell, 1986; Yamazaki *et al.* 2006).

The sweat rate on the dorsal foot was measured using a capacitance hygrometer (HygroFlex1; Rotronic Inst., Huntington, NY, USA). A small capsule was placed on the dorsal foot (0.79 cm^2 area) to detect sweating beside the laser Doppler probe to measure skin blood flow, and dry air was ventilated at 60 ml min^{-1} through the capsule.

HR, arterial pressures, and respiratory rate:

The HR was calculated from averaged R-R intervals of the ECG every minute. Systolic and diastolic arterial pressures were measured every minute via automated the right brachial artery auscultation to detect the Korotkoff sounds (model STBT-780, Colin, Komaki, Japan). The respiratory rate was calculated from the voluntary respiratory movement that was recorded using a respiratory belt transducer (MLT1132; AD Instruments, Colorado Springs, CO, USA).

RAV:

The RAV was determined from the images in the apical four-chamber view (**Fig. 1 A**) that were collected at ~24 frames per second (sampling rate = 23.7 Hz) for 5 cardiac cycles during each of the 10-min measurement periods using an ultrasound system (Vivid 7, General Electric, Fairfield, CT, USA). To calculate the RAV, the endocardial border of the right atrium was traced, whereas the areas of the right atrial appendage and superior/inferior vena cava were excluded. The long axis length of the right atrium was determined from the distance between the centre of the mitral annulus and the superior atrial wall. Next, the RAV was calculated using the monoplane area-length formula (DePace *et al.* 1983) for each frame as follows:

$$RAV = 8/3\pi \times (A^2/L),$$

where A is the right atrial endocardial area, and L is the long axis length, acquired from the apical four-chamber view. The peak RAV obtained from the volume wave every heartbeat were averaged (**Fig. 1 C**).

CCAD:

The CCAD was determined from the images of the right common carotid artery collected at ~14 frames per second (sampling rate = 14.1 Hz) for 5 cardiac cycles during each of the 10-min measurement periods using an ultrasound system (Vivid 7). To determine the CCAD, longitudinal images of the distal common carotid artery 1 cm proximal to the carotid bulb were acquired so that the interfaces of both the near and far wall were clearly visualised by placing the transducer perpendicular to the vessel wall (**Fig. 1 B**). Then, the perpendicular

distance from the adventitial-medial interface on the wall near the medial-adventitial interface on the far wall was measured every in frame (Tanaka *et al.* 2000). Typical examples are provided in **Fig. 1 C**. We defined a change in CCAD with the cardiac cycle as the ΔCCAD.

Data Acquisition

The rectified and filtered SSNA and MSNA signals, electrocardiographs (ECGs), skin blood flow, temperatures and relative humidities of the air flowing out of the capsule (used to calculate the sweat rate), and voluntary respiratory movements were recorded at a sampling rate of 200 Hz through an A/D converter using a computerised data-acquisition system (AD16-16U (PCI) EH; Contec, Tokyo, Japan). The skin temperatures and T_{oes} values were recorded every 30 sec with another A/D converter (34970A; Agilent Technologies, Santa Clara, CA, USA) and averaged every minute. The original SSNA and MSNA signals were recorded off-line from a digital tape recorder (RD-180T; TEAC, Tama, Japan) at 20 kHz after being passed through a band-pass filter of 700 – 2000 Hz as in previous studies (Kamijo *et al.* 2011).

Analyses

Mean blood pressure and cutaneous vascular conductance:

The pulse pressure (systolic blood pressure – diastolic blood pressure) and mean blood pressure (pulse pressure/3 + diastolic blood pressure) were calculated. The cutaneous vascular conductance (CVC) was calculated as the skin blood flow/mean arterial blood pressure and is presented as a percentage of the maximal CVC [%max]. To calculate the CVC on the dorsal foot in the head-up tilt position, we estimated the mean blood pressure in the dorsal foot by adding the hydrostatic pressure to the mean blood pressure of the right brachial artery at the heart level in the sitting position, whereas the hydrostatic pressure was estimated from the vertical distance from the foot to the right atrium. For 3 subjects, we confirmed that the estimated mean blood pressure (x) was identical to the mean blood pressure (y) of the anterior tibial artery as measured by the auscultation method (model STBT-780) on the dorsal foot during postural changes to positions of 15, 30, and 45° head-up-tilt (n=9, r=0.990, y=1.02x + 3.2, P<0.0001).

Total SSNA and MSNA:

Fig. 2 provides typical ECG and SSNA examples in the supine (*Left panels*) and MSNA in head-up tilt positions (*Right panels*) during hyperthermia from one subject. The raw signals were treated with a band pass filter (700 – 2000 Hz), and rectified and the filtered signals are illustrated from the top to the bottom of the figure. The peaks and leading and trailing edges of each SSNA or MSNA burst were identified from the trace of the rectified and filtered signals according to a previously described method (Rudas *et al.* 1999; Halliwill, 2000) with our modification (Okada *et al.* 2009; Kamijo *et al.* 2011) using a signal processing software (MATLAB 7.1; The MathWorks, Natick, MA, USA). Briefly, the burst amplitude was

obtained by subtracting the lower of the leading or trailing edge values from the peak value (amplitude = peak value - lower edge value). If the amplitude did not exceed a level two-fold higher than the baseline fluctuation of a 5- to 30-sec silent period with no bursts during normothermia, those data were excluded from the following analyses.

The burst area was determined by integrating the voltage every 1/200 sec from the time at the leading edge to the time at the trailing edge of each burst as given in the following formulae:

$$\text{area} = \frac{1}{200} \times \int_{t_{lead}}^{t_{trail}} A(t)dt \quad [\text{volts} \cdot \text{sec}],$$

where A(t) is the rectified and filtered SSNA or MSNA signal, and t_{lead} and t_{trail} are the times at the leading and trailing edges, respectively. The total SSNA or total MSNA per minute is expressed as follows:

$$\text{total SSNA or total MSNA} = \sum_{k=1}^{burst number/\,min} \text{area}(k) / \text{area}_{max} \times 100\% \ [\%\ \text{max min}^{-1}],$$

where the area_{max} is the maximal burst area determined in each subject in the normothermic and supine conditions. The same procedure was repeated every min of the 10-min measurement, and an average value per min in each condition was determined in each subject.

The SSNA and MSNA components that are synchronised with the cardiac cycle:

To determine the SSNA or MSNA components that were synchronised with the cardiac cycle, the original SSNA or MSNA spikes before rectification and filtering were analysed with a program that we developed by using the same signal processing software mentioned above. Briefly, we determined the standard deviation (SD) of the signals during the silent

periods with no apparent spikes for ~1.0 sec in the normothermic and supine conditions. Next, the SSNA or MSNA spikes with valleys below the threshold of the mean - 3 SD were chosen and used for the following spike incidence analyses. The reason we chose negative spikes is that the signals recorded with the electrode were extracellular potential, which should theoretically be negative.

Fig. 3 A illustrates a typical example of ECG signals and SSNA spikes over ~10 sec and the process by which the spike incidence histograms were made for every 5 sec. Briefly, a dataset of the original spikes of the SSNA for 5 sec after a given R wave of the ECG was chosen, the spike incidence of the SSNA was counted every 0.05 sec, and a histogram with 0.05-sec bins over 5 sec was constructed. The procedure was repeated for every R wave of the ECG over a given 1 min period to make ~60 histograms (HR per min; **Fig. 3 B)**. The histograms were averaged to create a histogram for 5 sec that served as the representative histogram of the spike incidence of the SSNA for the 1-min period **(Fig. 3 C)**. The same procedure was performed to make representative histograms of the R wave incidence and spike incidence of the MSNA for the 1-min period. Because the histograms were composed of periodic and non-periodic components, we defined the former as an upper area (UA) and the latter as a lower area (LA) on the boundary of the mean valley values of the periodic components for 5 sec **(Fig. 3 C)**.

We calculated the UA and LA per min (UA_{min} and LA_{min}, respectively) by multiplying the UA and LA for 5 sec by 60 sec/5 sec and also calculated the UA per one heartbeat (UA_{beat}) as the UA_{min} / HR (beats per min).

Latencies of the SSNA- and MSNA- components:

Fig. 4 depicts the profiles of the ECG, R-wave incidence histogram, RAV-wave, SSNA spike incidence histogram, CCAD-wave, and MSNA spike incidence histogram over 1.5 sec. The ECG-, RAV-, and CCAD- waves were redrawn from the period surrounded with grey-line squares in the lower panel of **Fig. 1 C.** An R-wave incidence histogram, and SSNA- and MSNA- spike incidence histograms were redrawn from the representative values for the given 1-min period surrounded by the grey-line squares in the lower panel of **Fig. 3 C**.

We defined the interval between the peaks of the R-wave incidence curve as T_R, and the interval between the peak incidences for the SSNA or MSNA components that were synchronized with the cardiac cycle as T_S. Additionally, we defined the latencies of the peak RAV and peak CCAD after an R wave of ECG as T_{RAV} and T_{CCAD}, respectively, and the latency of the peak of spike incidence for the SSNA or MSNA component after a peak incidence of R wave as T_{RS}.

We determined T_R and T_S by autocorrelation analysis, and additionally, we determined T_{RS} by cross-correlation analysis of the R-wave- incidence histogram and the SSNA- or MSNA-spike incidence histogram for a 5 sec period every minute after confirming that the correlation coefficients function at T_R, T_S, and T_{RS} reached the maximal values with significance (P<0.05). If we could not determine T_R, T_S, and T_{RS} in some periods according to the criteria, we interpolated the values at the closest time, but this situation accounted for only ~1% of all determinations.

Using the variables depicted in red in **Fig. 4,** we calculated the latency of the SSNA component after atrial distension from (T_{RS}-T_{RAV}) and that of the MSNA component after arterial deflation from (T_{RS}-T_{CCAD})**.**

The means and S.E.M. of T_R, T_S (**Fig. 6**), T_{RAV}, T_{CCAD}, T_{RS}, and the latencies of the SSNA and MSNA components for the 6 subjects (**Table 4**) are illustrated as representative values for the 10-min measurement period of each of 4 conditions; i.e., (normothermia vs. hyperthermia) × (supine vs. head-up tilt).

Statistics

Two-way [2 within (Condition: normothermia vs. hyperthermia) × (Posture: supine vs. head-up tilt)] ANOVA for repeated measures was used to identify any significant effects of passive warming and postural changes on thermoregulatory (**Table 1**) and cardiovascular responses (**Table 2**), SSNA and MSNA responses (**Table 3**), T_{RAV}, T_{CCAD}, and SSNA- and MSNA-T_{RS} (**Table 4**), and T_R and T_S. Additionally, to examine the significant differences in the changes in the variables due to postural change between the normothermia and hyperthermia conditions, we determined the (Condition × Posture) interaction effects on the variables in the analysis (**Tables 1-4, Fig. 5**). To examine any significant differences in the changes in CVC on the chest (CVC_{chest}) and on the dorsal foot (CVC_{foot}) due to postural change between the regions, two-way [2 within (Region: chest vs. foot) × (Condition)] ANOVA for repeated measures was used (**Fig. 5**).

Three-way [3 within (Condition) × (Posture) × (Nerve activity: SSNA vs. MSNA)] ANOVA was used to examine the significant differences in T_{RS} and latency in response to passive warming and postural change between the SSNA and MSNA (**Table 4**).

After confirming the significant differences with the ANOVAs, we used the Tukey-Kramer test as a subsequent post hoc test to determine any significant differences in the various pairwise comparisons. The standard least-squares method was used to determine the regression equations between T_R and T_S for SSNA and MSNA (**Fig. 6**) and also between UA_{min} for SSNA or MSNA and CVC_{chest} while the values in supine and head-up tilt position in both thermal conditions were pooled (**Fig. 7**). The statistical power ($1 - \beta$) is presented in the text at $\alpha = 0.05$ when the variables were significantly different between the postures or between the thermal conditions. All values are expressed as the means ± the S.E.Ms. except when noted. The null hypothesis was rejected at $P < 0.05$.

RESULTS

Table 1 displays the thermoregulatory responses to the postural change from the supine to the head-up tilt position in normothermia and hyperthermia in the 12 subjects together with the responses (enclosed in the parentheses) of the 6 subjects from whom SSNA and MSNA signals were simultaneously measured. In the 12 subjects, an increase in T_{oes} by ~0.7°C (P<0.0001, 1-β=1.0) after passive warming increased the sweat rate, CVC_{chest}, and CVC_{foot} (all, Ps<0.001, 1-β>0.99) in the supine position. The postural change from the supine to the head-up tilt position decreased the CVC_{chest} and CVC_{foot} in hyperthermia (both, Ps<0.013, 1-β>0.77) while in normothermia it decreased CVC_{foot} (P=0.0007, 1-β=0.99) but did not

decrease CVC_{chest} (P=0.86), and these decreases were followed by a ~0.1°C increase in the T_{oes} (both, Ps<0.0001, 1-β=1.0). In contrast, the sweat rate remained unchanged after the postural change in both thermal conditions (both, Ps>0.08). As stated in the table, the thermoregulatory responses to the postural change in the subset of data from the 6 subjects were almost similar to those in all 12 subjects.

Table 2 provides the HR, mean blood pressure, and pulse pressure responses of the 12 subjects in addition to the peak RAV and ΔCCAD responses of the 6 subjects to the postural change from the supine to head- up tilt position in both thermal conditions. In all 12 subject, an increase in T_{oes} decreased the peak RAV (P=0.0074, 1-β=0.94) in the supine position and increased the HR, pulse pressure, and ΔCCAD (all, Ps<0.04, 1-β>0.62). The postural change decreased the pulse pressure, peak RAV, and ΔCCAD in both thermal conditions (all, Ps<0.009, 1-β>0.84) and increased the HR and mean blood pressure (both, Ps<0.0001, 1-β=1.0). The postural change also elicited significant interaction effects [Condition × Posture] on the HR and mean blood pressure (both, Ps<0.011, 1-β>0.8), suggesting that the increase in mean blood pressure upon the postural change was attenuated, whereas the increase in HR was enhanced in hyperthermia compared with normothermia. Thus, the compensatory mechanisms function sufficiently such that no syncopal or near syncopal events occurred. As indicated in the table, the HR, mean blood pressure and pulse pressure responses to the postural change in the subset of data from the 6 subjects were almost similar to those in all 12 subjects.

Table 3 provides the SSNA and MSNA responses to the postural change from the supine to head-up tilt positon in both thermal conditions in the 6 subjects in whom both nerve

activities were simultaneously recorded. A rise in T_{oes} increased the total SSNA, total MSNA, SSNA-UA_{min}, and SSNA-LA_{min} in the supine position (all, *Ps*<0.015, *1-β*>0.84), but did not alter the other variables (all, *Ps*>0.05). In the hyperthermia condition, although the postural change increased the MSNA-UA_{min} (*P*=0.0367, *1-β*>0.62), it decreased the SSNA-UA_{min} (*P*=0.0168, *1-β*>0.8), and the SSNA-LA_{min} remained unchanged (*P*>0.76).

Fig. 5 summarises the changes in the peak RAV, ΔCCAD, total SSNA, total MSNA, SSNA-UA_{beat} and -UA_{min}, CVC_{chest}, and CVC_{foot} after the postural change in both thermal conditions. The values are presented as changes from the baselines before the postural change in both thermal conditions. The variables related to the SSNA and MSNA and the RAV, and ΔCCAD were taken from the 6 subjects, whereas the CVC_{chest}, and CVC_{foot} were taken from all 12 subjects. Although the changes in the peak RAV, ΔCCAD, total SSNA, total MSNA, and SSNA-UA_{beat} after the postural change were similar between the thermal conditions (all, *Ps*>0.29), the SSNA-UA_{min}, and CVC_{chest} decreased only in the hyperthermia condition (both, *Ps*<0.019, *1-β*>0.71), and the decrease in the CVC_{foot} was significantly greater than that in the CVC_{chest} (both, *Ps*<0.008, *1-β*>0.85).

Table 4 summarises the T_{RAV}, T_{CCAD}, SSNA- & MSNA-T_{RS}, and the latencies for the SSNA and MSNA components after a peak RAV and a valley of the ΔCCAD in the 6 subjects. A rise in T_{oes} decreased the T_{RAV} and MSNA-T_{RS} (both, *Ps*<0.008, *1-β*>0.94) with increased HR in the supine position, whereas it did not decrease the SSNA-T_{RS} (P>0.57). Similarly, the postural change decreased the T_{RAV} in both thermal conditions with increased HR (both, *Ps*<0.003, *1-β*>0.99). However, more importantly in the present study, the

SSNA-T_{RS} and the latency of the SSNA were shorter than those of the MSNA throughout the experiment (all, Ps<0.001, 1-β=1.0).

Fig. 6 illustrates the T_R vs. SSNA-T_S and MSNA-T_S relationships in the 6 subjects. As in the figure, the SSNA-T_S (y) and MSNA-T_S (y) were strongly correlated with the T_R (x) with regression equation of y=0.998x + 0.011 (r=1.00, P<0.0001) and y=1.045x – 0.019 (r=1.00, P=0.0002), respectively. Thus, the peak spike incidences of the SSNA and MSNA were synchronised with the cardiac cycle.

Fig. 7 illustrates the CVC_{chest} vs. SSNA-UA_{min} and MSNA-UA_{min} relationships in the 6 subjects, and the values in supine and head-up tilt positions in both thermal conditions were pooled. The SSNA-UA_{min} (x) was highly correlated with the CVC_{chest} (y) (r=0.817, P<0.0001, y=3.64x – 33.7) but the MSNA-UA_{min} was not (r=0.359, P=0.0853) while we confirmed that MSNA-UA_{min} was positively correlated with HR (r=0.603, P<0.002) and negatively with RAV_{peak} (r=-0.429, P<0.037) when the values in supine and head-up tilt positions in both thermal conditions were pooled across the 6 subjects. On the other hand, neither the SSNA-UA_{min} nor the MSNA-UA_{min} was significantly correlated with the CVC_{foot} (r=0.363, P=0.08 and r=0.041, P=0.849, respectively). The SSNA-LA_{min} (x) was significantly correlated with the sweat rate (y) on the dorsal foot (n=24, r=0.793, P<0.0001, y=0.004x – 0.06) when the values in supine and head-up tilt positions in both thermal conditions were pooled across the 6 subjects.

DISCUSSION

The major findings in the present study were as follows: 1) the SSNA-UA_{min}, an average SSNA component that was synchronised with the cardiac cycle per min, increased with T_{oes}, but this increase was suppressed when the posture was changed from the supine to the head-up tilt position; 2) the profile of the SSNA-UA_{min} during the warming and after the postural change was highly correlated with that of the CVC_{chest}, whereas the profile of the MSNA-UA_{min} was not, and 3) the latency of the SSNA component estimated from the time of the peak of SSNA spike incidence histogram after the peak RAV was ~40% shorter than that of the MSNA component estimated from the time of the peak of MSNA spike incidence histogram after a valley of the CCAD, which is consistent with the results of a previous study as follows (Fagius & Wallin, 1980).

Baroreflex control of SSNA-UA_{min} in hyperthermia:

Recently, Kamijo *et al*. (2011) examined the hypothesis that if the active vasodilator signals are evoked by the stretching of atrial receptors, they should be synchronised with the cardiac cycle because the afferent signals are generated synchronously with timing of the inflation and deflation of the atrium (Honig, 1981). Experimentally, Bini *et al*. (1981) suggested that SSNAs recorded from the posterior cutaneous antebrachial nerve include a component that was synchronised with the cardiac cycle in passively warmed subjects. Similarly, Macefield and Wallin (1996) suggested that the signals recorded from 3 of 8 single sudomotor fibres exhibited some latency after the R-wave time. Based on these results, Kamijo *et al*. (2011) analysed SSNA spikes according to the procedure illustrated in **Fig. 3**, and successfully identified the component that was synchronised with the cardiac cycle. These authors

confirmed that the component increased with an increase in T_{oes} during passive warming, but the response was suppressed during hypovolaemia. Because the profile of the component during passive warming was highly correlated with the CVC, these authors concluded that the component was the active vasodilator system and was modulated by baroreflexes to control skin blood flow during hyperthermia; however, it remains unknown whether the component works to maintain arterial pressure during postural changes from the supine to the upright position. On such occasions, more rapid response of the system is required.

Relationship between SSNA-UA_{min} and CVC_{chest} – compared to CVC_{foot} & venoarteriolar reflex:

In the present study, we reconfirmed that the SSNA component that was synchronised with the cardiac cycle as is the MSNA (**Fig. 6**) shared ~20% of the total signal in the supine position in hyperthermia (**Table 3**) as previously suggested (Kamijo *et al.* 2011). Moreover, as illustrated in **Fig. 5,** when the posture was changed from the supine to the head-up tilt position, the peak RAV and ΔCCAD decreased, the total SSNA remained unchanged, and the total MSNA increased to a similar extent in both thermal conditions. These findings are consistent with the results of previous studies that have demonstrated that the sensitivity of baroreflex control of the total MSNA remained unchanged, and the total SSNA does not change in response to unloading of the atrial or arterial baroreceptors during hyperthermia (Cui *et al.* 2002, 2004). In the present study, we found that the head-up tilt in hyperthermia decreased the SSNA-UA_{min} with decreases in the CVC_{chest}. Accordingly, as illustrated in **Fig. 7**, we found that the SSNA- UA_{min} was highly correlated with the CVC_{chest} whereas the

MSNA-UA_{min} was not. These results suggest that the component works to suppress cutaneous vasodilatation to maintain arterial pressure and possibly prevent a reduction in arterial pressure during postural changes in hot environments.

The CVC_{foot} decreased more than the CVC_{chest} upon postural change from the supine to the head-up tilt position in both thermal conditions in the 12 subjects (**Fig. 5**). Additionally, we found that the SSNA-UA_{min} was significantly correlated with the CVC_{chest} (**Fig. 7**) but not with the CVC_{foot}. This discrepancy might have been caused by the venoarteriolar reflex regulation of the skin blood flow in the head-up tilt position (Rowell, 1986; Yamazaki *et al.* 2006). The venoarteriolar reflex is induced by venous stasis via local sympathetic axon reflexes, i.e., when the venous pressure in a limb increases by over 25 mmHg, the muscular and cutaneous arteriolar resistances increase, and the blood flows decreases in the limb by ~40% (Rowell, 1986). The heart is at ~130 cm from the ground for a person who is 170 cm tall and standing upright. Thus, in the present study, in the 30° head-up tilt position, the hydrostatic pressure in the vein of the dorsal foot would be ~48 mmHg, which is sufficient to cause this reflex.

SSNA-UA_{min} latency:

As depicted in **Table 4,** the latency of the SSNA-component after a given peak RAV as calculated from (T_{RS}-T_{RAV}) was 0.65~0.83 sec, which is ~40% shorter than the 1.13~1.16 sec latency of the MSNA component after a given valley of the CCAD as calculated from (T_{RS}-T_{CCAD}). These findings are consistent with the previous results that demonstrated that the latency of a total SSNA burst after an arousal stimulation is 0.72-0.91 sec and ~40% shorter

than the 1.22-1.54 sec latency of an MSNA burst after a given R-wave on ECG in peroneal nerve recordings in subjects ~170 cm tall (Fagius & Wallin, 1980), similar to the heights in the present study. Thus, these results likely support the idea that the SSNA component is triggered by the stretch of atrial baroreceptors.

The reason for the slightly shorter latency of the SSNA component in the present study compared with that of the SSNA in the previous study (Fagius & Wallin, 1980) is that the conduction time of the afferent signals of the SSNA after an arousal stimulation might have been slightly longer than that after a peak RAV. Similarly, the reason for the shorter latency of the MSNA component in the present study compared with the MSNA latency in the previous study is that the conduction time for the afferent signals of the MSNA after an R-wave on ECG might have been slightly longer than that after a valley of the CCAD (**Table 4**).

What it means to heat syncope:

Heat syncope during the postural changes from the supine to the upright position is caused by a rapid fall in arterial blood pressure due to an insufficient compensatory responses against the decrease in total peripheral resistance due to systemic cutaneous vasodilatation and also against the reduction in venous return to the heart due to blood pooling in the cutaneous vein of the lower body (Lind *et al.* 1968). Regarding the feedback mechanisms for maintaining arterial pressure, although the baroreflex controls of the HR and MSNA are expected to work, the sensitivities of the reflexes remain unchanged in hyperthermia compared with those in normothermia (Yamazaki & Sone, 2001). Additionally, the α-adrenergic responsiveness of

the cutaneous vasculature is rather blunted in hyperthermia (Wilson *et al.* 2002), while this responsiveness in the muscular vasculature is unchanged (Cui *et al.* 2002). Thus, limited to these feedback mechanisms, humans do not appear to be specifically tolerant enough to be orthostatically challenged when exposed to a hot environment even though humans are unique in controlling body temperature by a large amount of skin blood flow and exercising in an upright position in contrast to other animal species.

To compensate for these factors, humans may have developed an active vasodilator system to control skin blood flow. The existence of this system has been broadly accepted based on the facts that hyperthermia–induced cutaneous vasodilatation in the forearm is abolished when the sympathetic nerves distributed in the area are blocked with a local anaesthetic (Edholm *et al.* 1957), and cutaneous vasodilatation is suppressed by a simulated orthostatic challenge with lower body negative pressure even after the active vasoconstrictor system is locally blocked by subcutaneous iontophoretic perfusion of an α-adrenergic antagonist (Kellogg *et al.* 1990). Additionally, there have been many studies that have suggested that atrial rather than arterial baroreceptors are involved in this suppression (Ahmad *et al.* 1977; Mack *et al.* 1988; Crandall *et al.* 1996; Nagashima *et al.* 1998). Thus, although the active vasodilator system likely significantly contributes to the prevention of heat syncope in humans, no studies have succeeded in recording the efferent signals of the reflex probably because the signals are too sparse to distinguish the signals from sudomotor signals. In the present study, we found that the SSNA-UA_{min} was at least one of the signals.

Limitation:

It is uncertain whether SSNAs recorded from the peroneal nerve reflect skin blood flow on the chest. However, Bini *et al*. (1980) reported that sympathetic neurograms recorded simultaneously from different nerves innervating the hairy skin, e.g., the superficial radial and the posterior cutaneous antebrachial nerves, exhibit strong synchrony in a moderately warm environments. Low *et al*. (2011) recorded SSNAs in the peroneal nerve and CVC on the dorsal forearm and suggested that the SSNA and cutaneous vasodilatation were both continuously increased as the body core temperature increased due to moderate to severe whole-body heating. Experimentally, we confirmed that the SSNA-UA_{min} vs. CVC_{chest} slope was identical to the SSNA-UA_{min} vs. CVC_{foot} slope in the semi-recumbent position in the previous study (Kamijo *et al.* 2011). Thus, the SSNAs recorded in the peroneal nerve reflect the SSNA that control skin blood flow on the chest with no influence from the venoarteriolar reflex.

In the present study, we used male subjects to avoid any effects of menstruation cycle on body temperature regulatory response to postural change (Minson *et al.* 2000; Tanaka *et al.* 2003). Further studies are needed to assess how the SSNA-UA_{min} response to posture change in female subjects.

Clinical Perspectives:

Recently, Cui *et al.* (2013) examined the total SSNA, CVC on the dorsal forearm, and sweat rate in response to passive warming in older patients with chronic heart failure and found that although the sweat rate and total SSNA responses were not significantly different from those of the age-matched control group, the CVC response was markedly attenuated.

Accordingly, these authors concluded that the attenuated cutaneous vasodilator response in heart failure patients was not attributable to a reduction in sympathetic outflow to the skin but was rather due to a reduced responsiveness of the skin vessels to the total SSNA. However, the results of the present study suggest another hypothesis, i.e., the attenuated cutaneous vasodilatation is at least in part caused by an attenuated increase in the SSNA-UA_{min} due to reduced sensitivity of the atrial baroreceptors with increased stiffness of the cardiac wall. In other words, if the cardiac compliance increases due to such as aerobic training (Arbab-Zadeh *et al.* 2004), the CVC response to hyperthermia and the baroreflex control of the CVC response will improve to prevent heat syncope.

In conclusion, the SSNA-component that is synchronised with the cardiac cycle activates the vasodilator system in response to hyperthermia and significantly contributes to the maintenance of arterial pressure during postural changes from the supine to the head-up tilt position probably via the unloading of atrial baroreceptors.

REFERENCES

Ahmad M, Blomqvist CG, Mullins CB & Willerson JT. (1977). Left ventricular function during lower body negative pressure. *Aviat Space Environ Med* **48,** 512-515.

Arbab-Zadeh A, Dijk E, Prasad A, Fu Q, Torres P, Zhang R, Thomas JD, Palmer D & Levine BD. (2004). Effect of aging and physical activity on left ventricular compliance. *Circulation* **110,** 1799-1805.

Bini G, Hagbarth KE, Hynninen P & Wallin BG. (1980). Regional similarities and differences in thermoregulatory vaso- and sudomotor tone. *J Physiol* **306,** 553-565.

Bini G, Hagbarth KE & Wallin BG. (1981). Cardiac rhythmicity of skin sympathetic activity recorded from peripheral nerves in man. *J Auton Nerv Syst* **4,** 17-24.

Crandall CG, Johnson JM, Kosiba WA & Kellogg DL, Jr. (1996). Baroreceptor control of the cutaneous active vasodilator system. *J Appl Physiol (1985)* **81,** 2192-2198.

Crandall CG, Shibasaki M & Wilson TE. (2010). Insufficient cutaneous vasoconstriction leading up to and during syncopal symptoms in the heat stressed human. *Am J Physiol Heart Circ Physiol* **299,** H1168-1173.

Crawshaw LI, Nadel ER, Stolwijk JA & Stamford BA. (1975). Effect of local cooling on sweating rate and cold sensation. *Pflugers Arch* **354,** 19-27.

Cui J, Boehmer JP, Blaha C, Lucking R, Kunselman AR & Sinoway LI. (2013). Chronic heart failure does not attenuate the total activity of sympathetic outflow to skin during whole-body heating. *Circ Heart Fail* **6,** 271-278.

Cui J, Wilson TE & Crandall CG. (2002). Baroreflex modulation of sympathetic nerve activity to muscle in heat-stressed humans. *Am J Physiol Regul Integr Comp Physiol* **282,** R252-258.

Cui J, Wilson TE & Crandall CG. (2004). Orthostatic challenge does not alter skin sympathetic nerve activity in heat-stressed humans. *Auton Neurosci* **116,** 54-61.

Delius W, Hagbarth KE, Hongell A & Wallin BG. (1972a). General characteristics of sympathetic activity in human muscle nerves. *Acta Physiol Scand* **84,** 65-81.

Delius W, Hagbarth KE, Hongell A & Wallin BG. (1972b). Manoeuvres affecting sympathetic outflow in human muscle nerves. *Acta Physiol Scand* **84,** 82-94.

Delius W, Hagbarth KE, Hongell A & Wallin BG. (1972c). Manoeuvres affecting sympathetic outflow in human skin nerves. *Acta Physiol Scand* **84,** 177-186.

DePace NL, Ren JF, Kotler MN, Mintz GS, Kimbiris D & Kalman P. (1983). Two-dimensional echocardiographic determination of right atrial emptying volume: a

noninvasive index in quantifying the degree of tricuspid regurgitation. *Am J Cardiol* **52,** 525-529.

Edholm OG, Fox RH & Macpherson RK. (1957). Vasomotor control of the cutaneous blood vessels in the human forearm. *J Physiol* **139,** 455-465.

Fagius J & Wallin BG. (1980). Sympathetic reflex latencies and conduction velocities in normal man. *J Neurol Sci* **47,** 433-448.

Halliwill JR. (2000). Segregated signal averaging of sympathetic baroreflex responses in humans. *J Appl Physiol* **88,** 767-773.

Honig CR. (1981). *Modern Cardiovascular Physiology*. Little, Brown and Company, Boston.

Kamijo Y, Okada Y, Ikegawa S, Okazaki K, Goto M & Nose H. (2011). Skin sympathetic nerve activity component synchronizing with cardiac cycle is involved in hypovolaemic suppression of cutaneous vasodilatation in hyperthermia. *J Physiol* **589,** 6231-6242.

Kellogg DL, Jr., Johnson JM & Kosiba WA. (1990). Baroreflex control of the cutaneous active vasodilator system in humans. *Circ Res* **66,** 1420-1426.

Kienbaum P, Karlssonn T, Sverrisdottir YB, Elam M & Wallin BG. (2001). Two sites for modulation of human sympathetic activity by arterial baroreceptors? *J Physiol* **531,** 861-869.

Lind AR, Leithead CS & McNicol GW. (1968). Cardiovascular changes during syncope induced by tilting men in the heat. *J Appl Physiol* **25,** 268-276.

Low DA, Keller DM, Wingo JE, Brothers RM & Crandall CG. (2011). Sympathetic nerve activity and whole body heat stress in humans. *J Appl Physiol (1985)* **111,** 1329-1334.

Macefield VG & Wallin BG. (1996). The discharge behaviour of single sympathetic neurones supplying human sweat glands. *J Auton Nerv Syst* **61,** 277-286.

Mack G, Nose H & Nadel ER. (1988). Role of cardiopulmonary baroreflexes during dynamic exercise. *J Appl Physiol (1985)* **65,** 1827-1832.

Minson CT, Halliwill JR, Young TM & Joyner MJ. (2000). Influence of the menstrual cycle on sympathetic activity, baroreflex sensitivity, and vascular transduction in young women. *Circulation* **101,** 862-868.

Nagashima K, Nose H, Takamata A & Morimoto T. (1998). Effect of continuous negative-pressure breathing on skin blood flow during exercise in a hot environment. *J Appl Physiol (1985)* **84,** 1845-1851.

Okada Y, Kamijo Y, Okazaki K, Masuki S, Goto M & Nose H. (2009). Pressor responses to isometric biting are evoked by somatosensory receptors in periodontal tissue in humans. *J Appl Physiol (1985)* **107,** 531-539.

Rowell LB. (1986). Human Circulation: Regulation During Physical Stress, pp. 1-416. Oxford University Press, New York.

Rudas L, Crossman AA, Morillo CA, Halliwill JR, Tahvanainen KU, Kuusela TA & Eckberg DL. (1999). Human sympathetic and vagal baroreflex responses to sequential nitroprusside and phenylephrine. *Am J Physiol* **276,** H1691-1698.

Tanaka H, Dinenno FA, Monahan KD, Clevenger CM, DeSouza CA & Seals DR. (2000). Aging, habitual exercise, and dynamic arterial compliance. *Circulation* **102,** 1270-1275.

Tanaka M, Sato M, Umehara S & Nishikawa T. (2003). Influence of menstrual cycle on baroreflex control of heart rate: comparison with male volunteers. *Am J Physiol Regul Integr Comp Physiol* **285,** R1091-1097.

Vallbo AB, Hagbarth KE, Torebjork HE & Wallin BG. (1979). Somatosensory, proprioceptive, and sympathetic activity in human peripheral nerves. *Physiol Rev* **59,** 919-957.

Wilson TE, Cui J & Crandall CG. (2002). Effect of whole-body and local heating on cutaneous vasoconstrictor responses in humans. *Auton Neurosci* **97,** 122-128.

Yamazaki F, Nakayama Y & Sone R. (2006). Whole-body heating decreases skin vascular response to low orthostatic stress in the lower extremities. *J Physiol Sci* **56,** 157-164.

Yamazaki F & Sone R. (2001). Thermal stress modulates arterial pressure variability and arterial baroreflex response of heart rate during head-up tilt in humans. *Eur J Appl Physiol* **84,** 350-357.

Author contributions

Y.O., Y.K., and H.N. conceived and designed the experiment. Y.O., Y.K., S.I., and S.M. contributed to data collection. Y.O., Y.K., S.M., and H.N. analysed the data and interpreted the experimental results. Y.O. drafted the manuscript. Y.K., S.M., and H.N. edited and revised the manuscript. All authors have approved the final version of the manuscript and agree to be accountable for all aspects of the work.

Acknowledgements

This work was supported in part by the grants from the Japan Society for the Promotion of Science (JP23590277 to Y.K. and JP24240089 to H.N.) and the Shinshu University Partnership Project between Shinshu University; Jukunen Taiikudaigaku Research Center; the Ministry of Education, Culture, Sports, Science, and Technology of Japan, and Matsumoto City.

Disclosures

None

FIGURE LEGENDS:

Fig. 1:

A: A typical image of the apical four-chamber view collected at ~24 frames per second using an ultrasound system. RA, right atrium; RV, right ventricle; LA, left atrium; LV, left ventricle. **B:** Typical images of the right common artery collected at ~14 frames per second using an ultrasound system in the supine (left) and head-up tilt (right) positions in hyperthermia. CCAD, common carotid arterial diameter determined as the perpendicular distance from the adventitial-medial interface on the near wall to the medial-adventitial interface on the far wall of the distal common carotid artery 1cm proximal to the carotid bulb. **C:** ECG, electrocardiograph; RAV, right atrial volume; CCAD waves for 4 cardiac cycles after a given R wave of an ECG at time zero.

Fig. 2:

ECG, raw, rectified, and filtered (integrated) spikes of the SSNA (left panel) and MSNA (right panel), respectively.

Fig. 3:

A: ECG (upper) and original SSNA recording and skin sympathetic nerve activity (bottom). **B:** R-wave and spike incidence of the SSNA histograms from the time of a given R-wave of the ECG in the 5-s windows with 0.05 s bins. The numbers 1, 2, 3…. on the histograms correspond to the numbers of 5-s windows in A. The procedure was repeated on every R wave of the ECG for a given 1 min period to create ~60 histograms (HR per min), and they were averaged to create a histogram for 5 sec as a representative histogram of the spike incidence of the SSNA for the 1-min period. A similar procedure was also performed on the R-waves and MSNAs. The UA (upper) and LA (lower) areas of the SSNA and MSNA are the components synchronised and non-synchronised with cardiac cycle, respectively, which were determined on the boundary of the mean valley values of the periodic components for 5 sec (**C**).

Fig. 4:

Electrocardiograph (ECG), R-wave incidence histogram, RAV-wave, SSNA spike incidence histogram, CCAD-wave, and MSNA spike incidence histogram. T_R, the interval between the peaks of the R wave incidence histogram; T_S, the interval between peaks of the SSNA or MSNA spike incidence histogram. T_{RAV} and T_{CCAD}, latencies of the peak of the RAV and the valley of the CCAD after an R wave of the ECG, respectively; T_{RS}, the latency of the peak of the spike incidence for an SSNA or MSNA after the peak incidence of the R wave; ΔCCAD, the change in CCAD with the cardiac cycle. The latencies of the SSNA and MSNA after arterial inflation and deflation, respectively, were calculated from (T_{RS}-T_{RA}) and (T_{RS}-T_{CCAD}), respectively. *, indicates that the average R-wave incidence histogram and the

SSNA and MSNA spike incidence histograms were obtained as average values over a minute by the procedure of calculation illustrated in **Fig. 3**.

Fig. 5:

RAV_{peak}, peak of the RAV wave; ΔCCAD, an amplitude of the common carotid arterial diameter; tSSNA, total SSNA; tMSNA, total MSNA; SSNA-UA_{beat}, upper area of the SSNA spike incidence histogram per heart beat; SSNA-UA_{min}, upper area of the SSNA spike incidence histogram per min; CVC_{chest}, cutaneous vascular conductance on the chest; and CVC_{foot}, cutaneous vascular conductance on the foot. The values are presented as changes from the baseline values before the postural change from the supine to the head-up tilt position. The means and S.E.M. bars for the 6 subjects with the SSNA or MSNA variables and the 12 subjects with the other cardiovascular variables. *, #, and Φ indicate significant differences from the base-line before the head-up tilt in each of the thermal conditions, between the thermal conditions, and from the CVC_{chest} at $P<0.05$, respectively.

Fig. 6:

The relationship between T_R, i.e., the interval between peaks of the R-wave incidence histogram, and T_S, i.e., the interval between the peaks of the SSNA (closed circles) or MSNA (open squares) spike incidence histogram. The symbols from the upper right to the left indicate the supine and tilt-up positions in normothermia and in hyperthermia in that order. The means and S.E.M. bars for 6 subjects are presented.

Fig. 7:

Relationships between UA_{min}, i.e., the upper area of the spike incidence histogram per min for the SSNA or MSNA, and CVC_{chest}, i.e., the cutaneous vascular conductance on the chest, in the supine and head-up tilt position in the normothermia and hyperthermia conditions, respectively. The data points for individual subjects are connected with dotted line arrows from the supine (○) to the head-up tilt position (●) in the normothermia and then from the supine (Δ) to the head-up tilt position (▲) in hyperthermia.

Table 1. Thermoregulatory responses during SUP and HUT in normothermia and hyperthermia

		Normothermia			Hyperthermia			*P* value		
	n	SUP	HUT		SUP	HUT		Condition	Posture	C × P
$\bar{T}_{sk}$, °C	12	34.9 ± 0.1	34.9 ± 0.1		36.9 ± 0.1 †	36.9 ± 0.1 †		<0.0001	n.s.	n.s.
	6	(34.8 ± 0.1)	(34.7 ± 0.1)		(37.0 ± 0.1) †	(37.0 ± 0.1) †		<0.0001	n.s.	n.s.
T_{oes}, °C	12	36.7 ± 0.1	36.7 ± 0.1	*	37.4 ± 0.0 †	37.5 ± 0.0	*†	<0.0001	<0.0001	0.0256
	6	(36.4 ± 0.1)	(36.5 ± 0.1)	*	(37.2 ± 0.1) †	(37.3 ± 0.1)	*†	0.0005	0.0104	n.s.
SR, mg min^{-1} cm^{-2}	12	0.04 ± 0.01	0.06 ± 0.01		0.29 ± 0.04 †	0.31 ± 0.04 †		0.0001	n.s.	n.s.
	6	(0.04 ± 0.02)	(0.05 ± 0.02)		(0.36 ± 0.07) †	(0.37 ± 0.07) †		0.0040	n.s.	n.s.

CVC, %max

CVC_{chest}	12	15.5	±	2.4	15.3	±	2.1		57.9	±	6.8	†	46.2	±	5.5	*†	<0.0001	0.0188	0.0115
	6	(17.7	±	4.1)	(16.6	±	2.9)		(62.2	±	6.0)	†	(50.6	±	5.6)	*†	0.0004	0.0248	0.0791
CVC_{foot}	12	11.5	±	2.2	4.1	±	1.3	*Φ	38.0	±	5.7	†Φ	13.7	±	2.9	*†Φ	0.0005	<0.0001	0.0016
	6	(10.5	±	3.6)	(2.3	±	0.8)		(38.5	±	7.2)	†Φ	(10.8	±	3.0)	*Φ	0.0072	0.0087	0.0465

$\bar{T}_{sk}$, mean skin temperature; T_{oes}, oesophageal temperature; SR, sweat rate; CVC_{chest} and CVC_{foot}, cutaneous vascular conductance of the chest and the foot, respectively. The values are presented as the means ± S.E.M. for the 12 subjects in the supine (SUP) and 30° head-up tilt (HUT) positions in the normothermic and hyperthermic conditions. The values enclosed in the parentheses are for the 6 subjects from whom SSNA and MSNA data were simultaneously recorded. Condition (normothermia vs. hyperthermia); Posture (SUP vs. HUT); C × P, the [Condition × Posture] interaction effect. *, $P < 0.05$ vs. SUP; †, $P < 0.05$ vs. normothermia; Φ, $P < 0.05$ vs. CVC_{chest}.

Table 2. Cardiovascular responses during SUP and HUT in normothermia and hyperthermia

		Normothermia			Hyperthermia			*P* value		
	n	SUP	HUT		SUP	HUT		Condition	Posture	C × P
HR, beats min^{-1}	12	59 ± 2	62 ± 2 *		81 ± 2 †	91 ± 2 *†		<0.0001	<0.0001	<0.0001
	6	(56 ± 3)	(61 ± 3) *		(81 ± 3) †	(92 ± 3) *†		0.0003	0.0011	0.0208
MBP, mmHg	12	85 ± 2	91 ± 2 *		85 ± 2	88 ± 2 *		n.s.	<0.0001	0.0106
	6	(85 ± 3)	(91 ± 4) *		(86 ± 2)	(88 ± 2) *		n.s.	0.0080	n.s.
PP, mmHg	12	52 ± 3	48 ± 2 *		65 ± 4 †	61 ± 4 *†		0.0003	0.0082	n.s.
	6	(51 ± 5)	(47 ± 4)		(65 ± 6) †	(63 ± 8) †		0.0095	n.s.	n.s.
RAV_{peak}, ml	6	50 ± 5	38 ± 3 *		37 ± 4 †	25 ± 3 *†		<0.0001	0.0074	n.s.
ΔCCAD, mm	6	0.70 ± 0.06	0.59 ± 0.05 *		0.78 ± 0.07 †	0.64 ± 0.06 *		0.0370	0.0059	n.s.

HR, heart rate; MBP, mean blood pressure; PP, pulse pressure for all 12 subjects in the supine (SUP) and 30° head-up tilt (HUT) positions in the normothermic and hyperthermic conditions. The values enclosed in the parentheses are for the 6 subjects from whom SSNA and MSNA data were

simultaneously recorded. RAV_{peak}, the peak of right atrial volume cycle; ΔCCAD, the amplitude of the common carotid arterial diameter for the 6 subjects. The values are presented as the means ± S.E.M. Condition (normothermia vs. hyperthermia); Posture (SUP vs. HUT); C × P, the [Condition × Posture] interaction effect. *, $P < 0.05$ vs. SUP; †, $P < 0.05$ vs. normothermia.

Table 3. tSSNA, tMSNA, and UA and LA for SSNA and MSNA during SUP and HUT in normothermia and hyperthermia

	Normothermia		Hyperthermia		*P* value		
	SUP	HUT	SUP	HUT	Condition	Posture	C × P
tSSNA, %max min^{-1}	3.49 ± 0.57	4.27 ± 0.67	8.31 ± 0.46 †	8.52 ± 0.54 †	0.0043	n.s.	n.s.
tMSNA, %max min^{-1}	927 ± 124	1195 ± 146 *	1530 ± 127 †	1841 ± 123 *†	0.0068	0.0373	n.s.
SSNA							
UA_{min}, counts min^{-1}	17.5 ± 2.1	15.5 ± 1.6	24.3 ± 1.6 †	20.2 ± 1.7 *†	0.0141	0.0168	n.s.
UA_{beat}, counts $beat^{-1}$	0.33 ± 0.05	0.26 ± 0.04 *	0.31 ± 0.03	0.22 ± 0.02 *	n.s.	0.0094	n.s.

LA_{min}, counts min^{-1}	36.1	±	6.3	36.9	±	5.8	109.4	±	12.7 †	112.9	±	13.1 †	0.0005	n.s.	n.s.
MSNA															
UA_{min}, counts min^{-1}	20.5	±	2.9	32.4	±	5.4	35.4	±	3.8	52.6	±	7.8 *	n.s.	0.0367	n.s.
UA_{beat}, counts $beat^{-1}$	0.39	±	0.06	0.53	±	0.08	0.45	±	0.05	0.58	±	0.09	n.s.	n.s.	n.s.
LA_{min}, counts min^{-1}	35.0	±	9.4	44.4	±	6.8	42.4	±	11.5	84.9	±	32.0	n.s.	n.s.	n.s.

tSSNA, total SSNA; tMSNA, total MSNA; UA_{min}, upper area; UA_{beat}, upper area per heart beat; LA_{min}, lower area. The values are presented as the means ± S.E.M. for the 6 subjects from whom SSNA and MSNA data were simultaneously recorded in the supine (SUP) and 30° head-up tilt (HUT) positions in the normothermic and hyperthermic conditions. Condition (normothermia vs. hyperthermia); Posture (SUP vs. HUT); C × P, the [Condition × Posture] interaction effect. *, $P < 0.05$ vs. SUP; †, $P < 0.05$ vs. normothermia.

Table 4. T_{RAV}, T_{CCAD}, and T_{RS} and conduction time for SSNA and MSNA during SUP and HUT in normothermia and hyperthermia

	Normothermia			Hyperthermia			*P* value		
	SUP	HUT		SUP	HUT		Condition	Posture	C × P
T_{RAV}, sec	0.39 ± 0.01	0.35 ± 0.00	*	0.31 ± 0.01	†	0.25 ± 0.01	*†	<0.0001	0.0021	n.s.
T_{CCAD}, sec	0.07 ± 0.01	0.08 ± 0.01		0.05 ± 0.01		0.06 ± 0.01		n.s.	n.s.	n.s.
T_{RS}, sec										
SSNA	1.04 ± 0.03	1.06 ± 0.06		1.08 ± 0.03		1.08 ± 0.05		n.s.	n.s.	n.s.
MSNA	1.23 ± 0.02	§ 1.24 ± 0.02	§	1.20 ± 0.02	†§	1.19 ± 0.02	†§	0.0071	n.s.	n.s.
Latencies, sec										
SSNA	0.65 ± 0.03	0.71 ± 0.06		0.76 ± 0.04		0.83 ± 0.05		n.s.	n.s.	n.s.
MSNA	1.16 ± 0.02	‡ 1.16 ± 0.02	‡	1.15 ± 0.01	‡	1.13 ± 0.02	‡	n.s.	n.s.	n.s.

T_{RAV}, latency of the first peak of the right atrial volume wave after an R-wave; T_{CCAD}, latency of the first valley of the common carotid artery diameter wave after an R-wave; T_{RS}, time at the peak of the spike incidence after an R-wave. The latencies of the SSNA and MSNA were calculated as (T_{RS} - T_{RAV}) and (T_{RS}

- T_{CCAD}), respectively. The values are presented as the means ± S.E.M. for the 6 subjects from whom the SSNA and MSNA were simultaneously recorded in the supine (SUP) and 30° head-up tilt (HUT) positions in the normothermic and hyperthermic conditions. Condition (normothermia vs. hyperthermia); Posture (SUP vs. HUT); C × P, the [Condition × Posture] interaction effect. *, $P < 0.05$ vs. SUP; †, $P < 0.05$ vs. normothermia; §, $P < 0.05$ vs. T_{RS} for SSNA; ‡, $P < 0.05$ vs. SSNA conduction time.

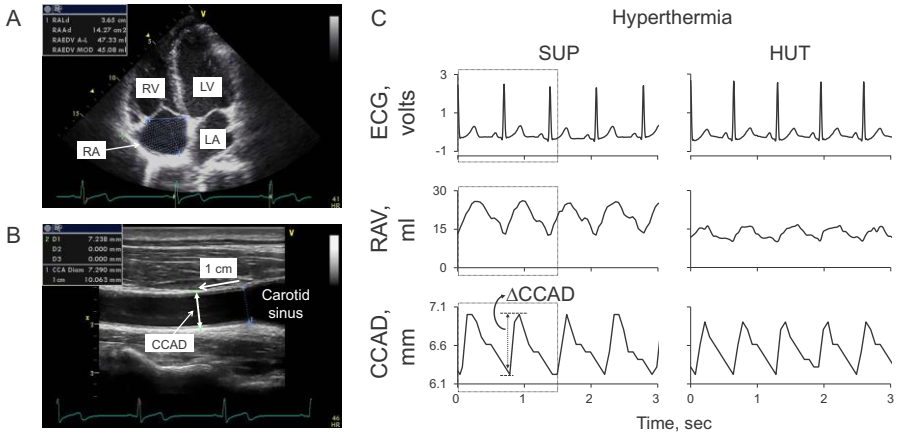

Figure 1

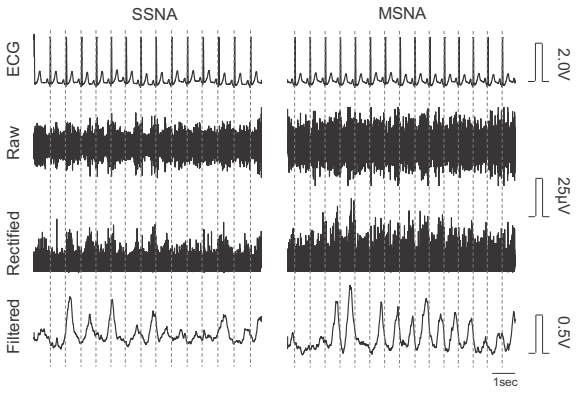

Figure 2

This is an Accepted Article that has been peer-reviewed and approved for publication in the The Journal of Physiology, but has yet to undergo copy-editing and proof correction. Please cite this article as an 'Accepted Article'; doi: 10.1113/JP273281.

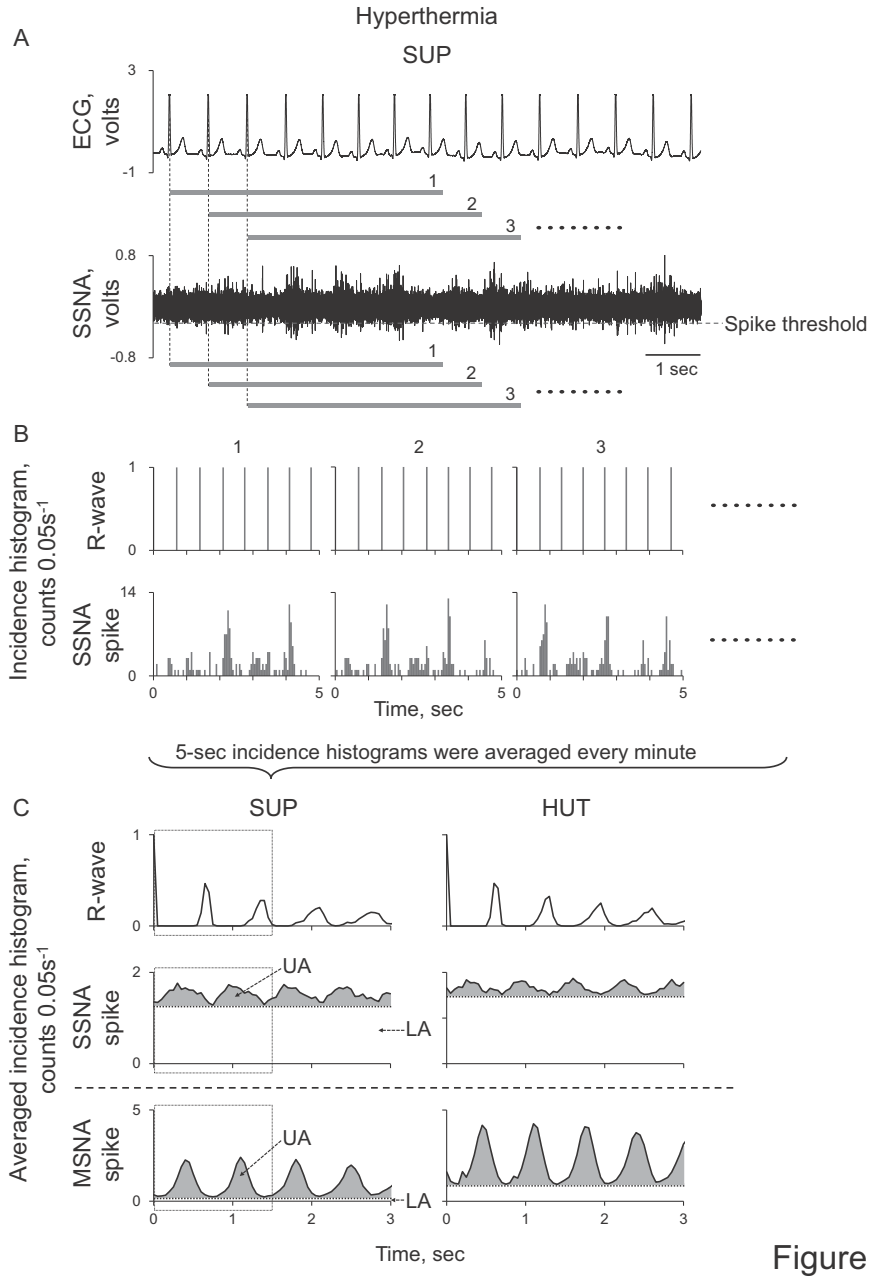

Figure 3

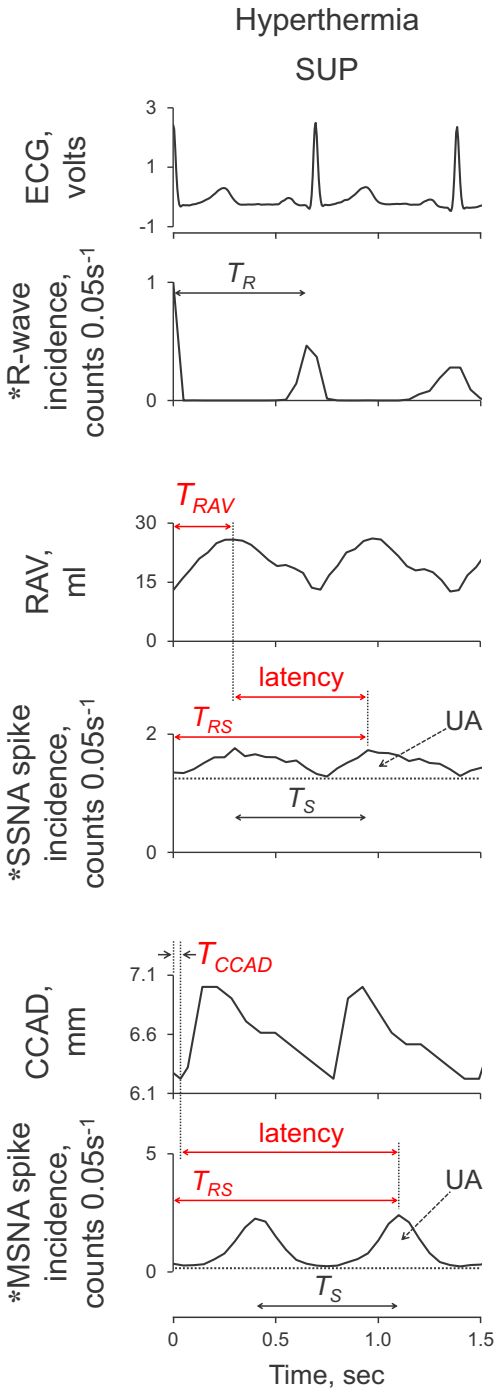

Figure 4

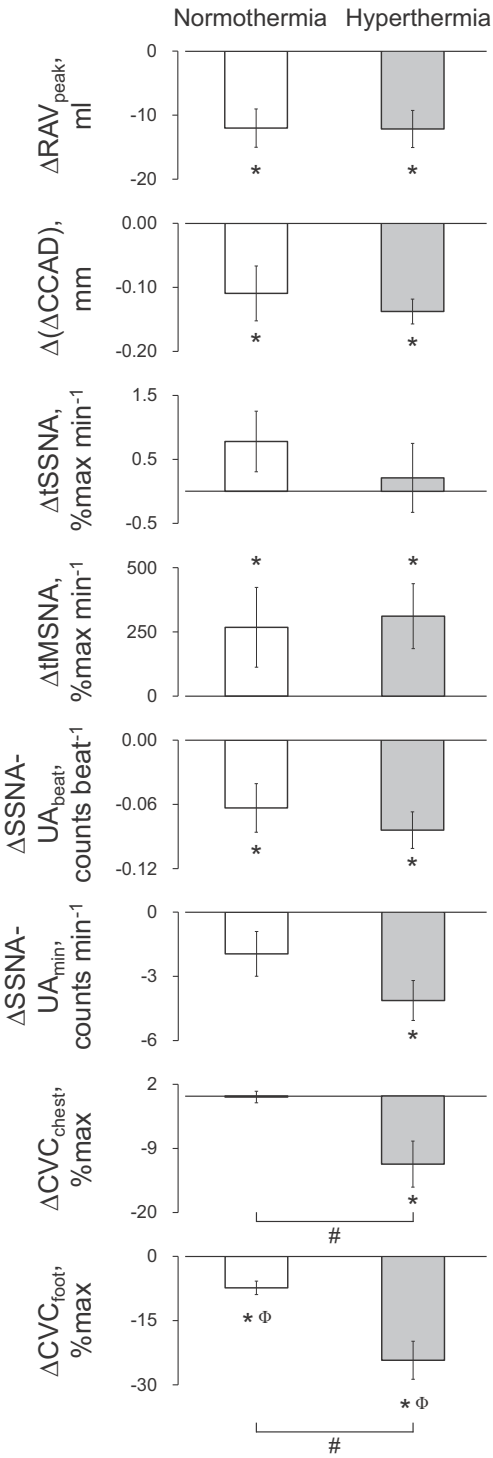

Figure 5

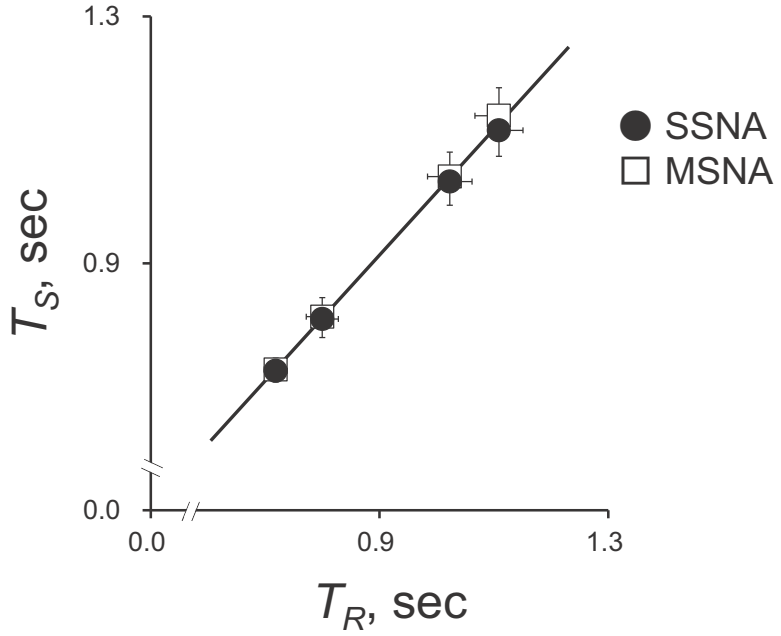

Figure 6

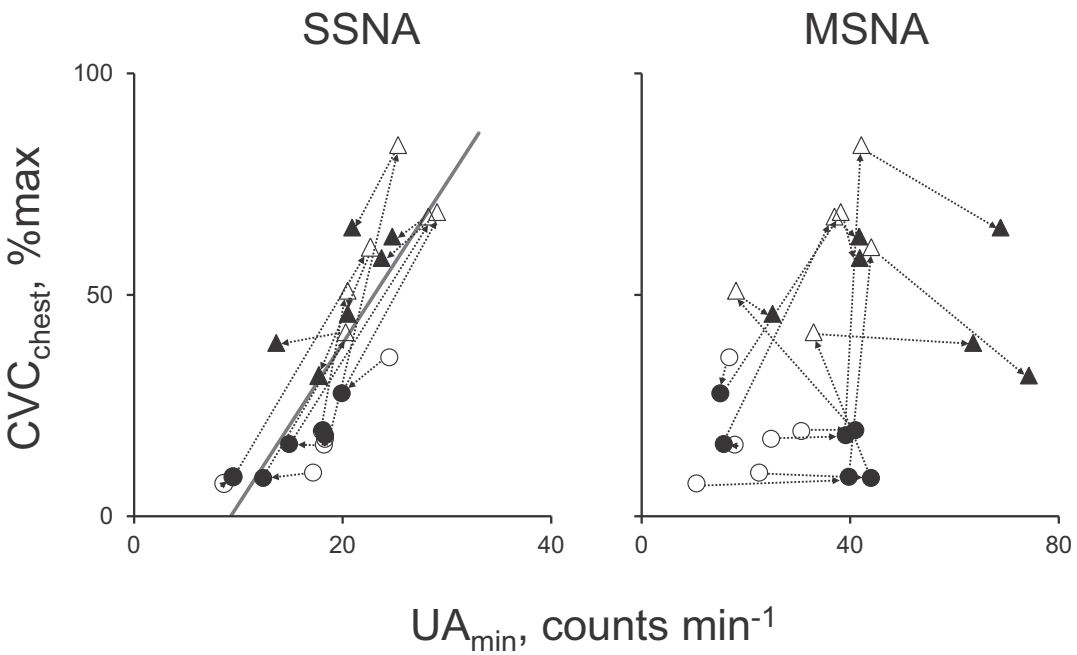

Figure 7